BNL-94605-2011-TECH

BNL-94605-2011-IR

Source of second order chromaticity in RHIC

Y. Luo,

January 2011

Collider Accelerator Department

Brookhaven National Laboratory

U.S. Department of Energy

USDOE Office of Science (SC)

DISCLAIMER

BNL-94605-2011-IR

C-A/AP/#418
Jan. 2011

Source of Second Order Chromaticity in RHIC

Y. Luo, X. Gu, W. Fischer, and D. Trbojevic

Collider-Accelerator Department
Brookhaven National Laboratory
Upton, NY 11973

January 20, 2011

Source of second order chromaticity in RHIC

Y. Luo, X. Gu, W. Fischer, and D. Trbojevic
Brookhaven National Laboratory, Upton, NY 11973, USA

In this note we will answer the following questions: 1) what is the source of second order chromaticities in RHIC? 2) what is the dependence of second order chromaticity on the on-momentum β-beat? 3) what is the dependence of second order chromaticity on β^* at IP6 and IP8? To answer these questions, we use the perturbation theory to numerically calculate the contributions of each quadrupole and sextupole to the first, second, and third order chromaticities.

1 Perturbation Theory

Based on the perturbation theory [1], the horizontal and vertical betatron tune changes due to a small quadrupole error $\Delta k_1(s)$ are

$$\Delta Q_{x,y} = \pm\frac{1}{4\pi}\oint \beta_{x,y}(s)\Delta k_1(s)ds. \tag{1}$$

where $\beta_{x,y}(s)$ are the unperturbed horizontal and vertical amplitude functions.

The off-momentum tune shifts are

$$\Delta Q_{x,y} = \xi^{(1)}_{x,y}\delta + \xi^{(2)}_{x,y}\delta^2 + \xi^{(3)}_{x,y}\delta^3... \tag{2}$$

where $\delta = \Delta p/p_0$. The first define the first, second, and third order chromaticities are

$$\xi^{(1)}_{x,y} = \frac{\partial Q_{x,y}}{\partial\delta}, \tag{3}$$

$$\xi^{(2)}_{x,y} = \frac{1}{2}\frac{\partial^2 Q_{x,y}}{\partial\delta^2}, \tag{4}$$

$$\xi^{(3)}_{x,y} = \frac{1}{6}\frac{\partial^3 Q_{x,y}}{\partial\delta^3}. \tag{5}$$

For an off-momentum particle, $\Delta k_1(s)$ in Eq. (1) from quadrupoles and sextupoles is given by

$$\begin{aligned}\Delta k_1(s)_{x,y} &= [\pm K_1(s) \mp K_2(s)D_x(s)](\tfrac{1}{1+\delta}-1)\\ &= [\mp K_1(s) \pm K_2(s)D_x(s)](\delta-\delta^2+\delta^3-\delta^4+....),\end{aligned} \tag{6}$$

where K_1 and K_2 are the nominal strengths of quadrupoles and sextupoles, $D_x(s)$ is the horizontal dispersion.

Plugging Eq. (6) into Eq. (1) and only keep the terms of δ, we obtain the first order chromaticities

$$\xi^{(1)}_{x,y} = \frac{1}{4\pi}\oint \beta_{x,y}(s)[\mp K_1(s) \pm K_2(s)D_x(s)]ds. \tag{7}$$

Take derivative of Eq. (7) with respect to δ and keep the terms of δ^2 in Eq. (6), we obtain the second order chromaticities [2]

$$\xi^{(2)}_{x,y} = -\frac{1}{2}\xi^{(1)}_{x,y} + \frac{1}{8\pi}\oint[\mp K_1 \pm K_2D_x]\frac{\partial\beta_{x,y}}{\partial\delta}ds + \frac{1}{8\pi}\oint \pm K_2\beta_{x,y}D^{(2)}_x ds. \tag{8}$$

Similarly, the third order chromaticities are

$$\begin{aligned}\xi^{(3)}_{x,y} &= -\tfrac{1}{3}\xi^{(2)}_{x,y} + \tfrac{1}{24\pi}\oint[\mp K_1 \pm K_2D_x]\tfrac{\partial^2\beta_{x,y}}{\partial\delta^2}ds + \tfrac{1}{24\pi}\oint[\pm K_1 \mp K_2D_x]\tfrac{\partial\beta_{x,y}}{\partial\delta}ds\\ &+\tfrac{1}{24\pi}\oint[\pm K_2D^{(2)}_x]\tfrac{\partial\beta_{x,y}}{\partial\delta}ds + \tfrac{1}{24\pi}\oint[\pm K_2D^{(3)}_x]\beta_{x,y}ds\\ &+\tfrac{1}{24\pi}\oint[\mp K_2D^{(2)}_x]\beta_{x,y}ds + \tfrac{1}{24\pi}\oint \pm K_2D^{(2)}_x\tfrac{\partial\beta_{x,y}}{\partial\delta}ds.\end{aligned} \tag{9}$$

where we defined $D_x = \frac{\partial x_{co}}{\partial\delta}$, $D^{(2)}_x = \frac{\partial^2 x_{co}}{\partial\delta^2}$, and $D^{(3)}_x = \frac{\partial^3 x_{co}}{\partial\delta^3}$.

2 Sources of chromaticities

In this section, we will use the above Eqs. (6)-(8) to search the sources of second order chromaticities. In our studies, the 2009 RHIC 100 GeV polarized proton (p-p) run Blue ring lattice, the 2011 RHIC 250 GeV p-p run Blue ring lattice, and the 2010 RHIC 100 GeV Au-Au run Yellow ring lattice are used. For the 2009 RHIC 100 GeV p-p run Blue ring lattice and the 2010 RHIC 100 GeV Au-Au run Yellow ring lattice, the nominal β^* at IP6 and IP8 is 0.7 m. For the 2011 RHIC 250 GeV p-p run Blue ring lattice, the nominal β^* at IP6 and IP8 is 0.65 m.

2.1 Examples

Figure 1 shows the horizontal dispersion D_x along the ring for the 2009 RHIC 100 GeV p-p run Blue ring lattice and the 2011 RHIC 250 GeV p-p run Blue lattice. From Figure 1, the dispersion in the interaction region (IR) IR6 and IR8 of the 2011 RHIC 250 GeV p-p run Blue ring lattice is much bigger than that of the 2009 RHIC 100 GeV p-p run Blue ring lattice.

Figure 2 shows the horizontal off-momentum β-beat $\frac{\partial \beta_x}{\partial \delta}$ along the ring for the 2009 RHIC 100 GeV p-p run Blue ring lattice and the 2011 RHIC 250 GeV p-p run Blue ring lattice. For the 2009 RHIC 100 GeV p-p run Blue ring lattice, the amplitude of the horizontal off-momentum β-beats in IR6 and IR8 are comparable. However, for the 2011 RHIC 250 GeV p-p run Blue ring lattice, the horizontal off-momentum β-beat in IR8 is almost twice than that in IR6. From Eq. (7), the off-momentum β-beat plays a crucial role in the second order chromaticity contribution.

Based on Eqs. (6)-(8), we are able to calculate each quadruple or sextupole's contributions to the first, second, and third chromaticities. As an example, Figure 3 shows the contributions from each element to the first order horizontal chromaticity $\xi_x^{(1)}$. In this example, the 2011 RHIC 250 GeV p-p run Blue ring lattice is used. The first order chromaticities are not corrected.

2.2 Sources

To localize the sources of chromaticities, the first order chromaticities are not corrected. The uncorreced horizontal and vertical chromaticities are (-89.8, 87.1), (-95.2, -94.0), and (-95.6, -101.3) for the 2009 RHIC 100 GeV p-p run Blue ring lattice, the 2011 RHIC 250 GeV p-p run Blue ring lattice, and the 2010 RHIC 100 GeV Au-Au run Yellow ring lattice.

Tables 1-3 list the contributions of each sections to the first, second and third order chromaticities for the above three lattices. The sections include 6 IRs and 6 arcs. We define each arc is between Q9 and Q9. Q9s is included in IRs.

Table 4 summarizes each section's contributions in percentage to the whole ring for the three above lattices. The percentage is defined as the contribution of one section divided by the absolute value of the whole ring's value. Figures 4-6 plot each section's contributions in percentage for the above three lattices.

From Table 4, IR6 and IR8 contribute about 47%-58% to the first order chromaticities, while the 4 non-colliding IRs contribute about 20%-26% and 6 arcs contribute about 21%-25%.

From Table 4, more than 90% of contributions to the second order chromaticities are from IRs. The contributions from 6 arcs are quite small. IR6 and IR8 contribute about 185% and 120% to the horizonatal second order chromaticity for the 2009 and 2011 p-p run lattices, while the non-colliding IRs contribute about -77% and -20%. For the vertical second order chromaticity, IR6 and IR8 contribute 78% and 84% for 2009 and 2011 run lattices, while the non-colliding IRs contribute about 24% and 17%. For the 2010 Au-Au run Yellow lattice, IR6 and IR8 contribute 34% and 115% to the horizontal and vertical second order chromaticity, while the other IRs contribute 71% and -20%.

Also from Table 4, IR6 and IR8 contribute about 71% - 86% to the third order chromaticities. The non-colliding IRs contribute about 16% except 3% in the vertical plane for the 2010 Au-Au run Yellow lattice. For all three lattices, less than 11% of the third order chromaticities are contributed by the arcs.

Table 1: Section contributions to chromaticities with 2009 250GeV p-p run Blue ring lattice ($\xi^{(1)}$ uncorr.)

	$\xi_x^{(1)}$	$\xi_y^{(1)}$	$\xi_x^{(2)}$	$\xi_y^{(2)}$	$\xi_x^{(3)}$	$\xi_y^{(3)}$
IR6	-24.82	-23.33	810.26	1466.45	-531496	-442262
ARC0608	-3.62	-3.37	2.47	-49.23	-2849.05	-14452.4
IR8	-24.82	-23.33	811.6	1462.74	-530935	-442788
ARC0810	-3.18	-3.77	-25.01	6.07	-36950.6	-16592.3
IR10	-4.95	-4.74	-293.83	191.45	-62204.2	-57063
ARC1012	-3.62	-3.37	12.03	-37.72	-28244.2	-13300.2
IR12	-4.92	-4.74	-47.23	272.35	-65457	-53276.3
ARC1202	-3.18	-3.77	-41.55	5.64	-39509.9	-23153
IR2	-4.92	-4.74	-47.31	272.46	-65546.7	-53258.8
ARC0204	-3.62	-3.37	12.03	-37.82	-28236.2	-13362.7
IR4	-4.95	-4.74	-293.69	191.88	-62151.4	-57005.4
ARC0406	-3.18	-3.77	-25.06	6.12	-36963.9	-16659.7
SUM	-89.82	-87.09	874.69	3750.41	-1.49054e+06	-1.20317e+06

Table 2: Section contributions to chromaticities for 2011 250GeV p-p run Blue ring lattice ($\xi^{(1)}$ uncorr.)

	$\xi_x^{(1)}$	$\xi_y^{(1)}$	$\xi_x^{(2)}$	$\xi_y^{(2)}$	$\xi_x^{(3)}$	$\xi_y^{(3)}$
IR6	-27.58	-27.03	1041.71	1712	-658670	-560237
ARC0608	-3.57	-3.3	-4.11	-54.07	-11388.5	-40198.8
IR8	-27.96	-26.79	1629.69	1633.69	-551647	-545354
ARC0810	-3.14	-3.72	-8.55	3.01	-36019.1	-9845.38
IR10	-4.17	-4.05	-220.9	86.62	-51924.5	-34472.2
ARC1012	-3.58	-3.31	30.37	-26.74	-35417.6	-3097.39
IR12	-4.18	-4.05	-146.84	127.5	-52203.1	-42809.9
ARC1202	-3.13	-3.72	-22.5	0.83	-38012	-11074.9
IR2	-6.94	-6.86	83.58	392.44	-109158	-116487
ARC0204	-3.58	-3.3	20.27	-25.63	-21679.4	-4756.59
IR4	-4.2	-4.06	-178.06	90.99	-33438.8	-35674.1
ARC0406	-3.14	-3.72	-12.79	5.62	-26344.3	-11675.7
SUM	-95.2	-93.97	2211.86	3946.29	-1.6259e+06	-1.41568e+06

Table 3: Section contributions to chromaticities for 2010 100GeV Au-Au run Yellow ring lattice ($\xi^{(1)}$ uncorr.)

	$\xi_x^{(1)}$	$\xi_y^{(1)}$	$\xi_x^{(2)}$	$\xi_y^{(2)}$	$\xi_x^{(3)}$	$\xi_y^{(3)}$
IR6	-22.87	-25.61	522	1339.18	-811593	-707616
ARC0604	-4.29	-4.01	-58.23	4.26	-47003.6	-40115.2
IR4	-6.46	-6.08	508.78	-315.65	-77687	-7660.6
ARC0402	-3.76	-4.48	-16.44	35.25	-34501.8	-35505.5
IR2	-6.34	-6.19	584.75	81.2	-109208	-23254.2
ARC0212	-4.27	-4.02	-33.49	30.17	-38995	-18309.4
IR12	-6.34	-6.19	584.89	84.05	-109397	-21279.2
ARC1210	-3.76	-4.48	-16.47	34.84	-34433.6	-35053.8
IR10	-6.46	-6.08	506.54	-311	-74223.3	-8811.74
ARC1008	-4.29	-4.01	-57.96	4.13	-49181.6	-37313.3
IR8	-22.87	-25.61	521.65	1317.19	-811990	-716451
ARC0806	-3.82	-4.47	-5.9	-11.08	24394.9	-2039.15
SUM	-95.58	-101.3	3040.12	2292.57	-2.17382e+06	-1.65341e+06

2.3 Summary

In summary, for the above three lattices, IR6 and IR8 contributed about 50% or more to the first order chromaticities and more than 70% to the third order chromaticities. IRs contribute more than 90% to the

Table 4: Contributions to the linear and nonlinear chromaticities

Sections	$\xi_x^{(1)}$	$\xi_y^{(1)}$	$\xi_x^{(2)}$	$\xi_y^{(2)}$	$\xi_x^{(3)}$	$\xi_y^{(3)}$
2009-pp-Blue:						
IR6 and IR8	-0.55	-0.53	1.85	0.78	-0.71	-0.73
Other IRs	-0.21	-0.21	-0.77	0.24	-0.17	-0.18
Arcs	-0.22	-0.24	-0.07	-0.02	-0.11	-0.081
2011-pp-Blue:						
IR6 and IR8	-0.58	-0.57	1.20	0.84	-0.74	-0.78
Other IRs	-0.20	-0.20	-0.20	0.17	-0.15	-0.16
Arcs	-0.21	-0.22	0.00	-0.02	-0.10	-0.05
2010-AuAu-Yellow:						
IR6 and IR8	-0.47	-0.50	0.34	1.15	-0.74	-0.86
Other IRs	-0.26	-0.24	0.71	-0.20	-0.17	-0.03
Arcs	-0.25	-0.25	-0.06	0.04	-0.08	-0.10

second order chromaticities. For the p-p run lattices, IR6 and IR8 contribute 185% and 120% of the total horizontal second order chromaticity for 2009 and 2011 run lattices. The non-colliding IRs contribute -77% and -20%. For the 2010 Au-Au run Yellow ring lattice, each IR contribute about 20% to the horizontal second order chromaticity. IR6 and IR8 contributes about 120% to the vertical chromaticity. For the $\xi_{x,y}^{(1)}$ uncorrected lattices, the arcs contribute about 20% to the first order chromaticities. However, their contributions to the second and third order chromaticities are small.

As a comparison, Tables 5-7 list the contributions of each sections to the first, second and third order chromaticities for the above three lattices with first order chromaticities corrected to (1,1). In the correction, all focusing and defocusing sextupoles have the same strengths. Comparing Tables 1-3 and Tables 5-7, After first order chromaticity correction, the second order chromaticities do not change too much. This can be explained by the fact that the betatron phase advance of each FODO cell in the RHIC arcs are about 90° [3]. The adjacent sextupoles' contribution to the second order chromaticity will cancel.

3 Nonlinear chromaticity's dependence on on-momentum β-beat

In this section, we will investigate the effects of on-momentum β-beat on the second order chromaticities. The on-momentum β-beat is the β change of on-momentum particles due to quadrupole errors.

3.1 Simulation Setup

In the following simulation study, we will randomly assign strength errors to all the quadroples to generate on-momentum β-beat. The quadrupole errors are given in percentage. The error percentage are generated with the formula $MaxErr * (rnd(1) - 0.5) * 2$, where function $rnd(1)$ is the random number generator which produces random numbers with a uniform distribution between (0-1), $MaxErr$ is maximum strength error in percentage. For each seed or case, we keep $MaxErr$ same for all quadrupoles. In this study, $MaxErr$ is chosen to be 0.0005, 0.001, 0.002, 0.003, 0.004. We simulate 50 sets of quadrupole errors for each lattice. The first order chromaticities are corrected to (+1, +1).

We will focus on the averaged on-momentum β-beat $< \Delta\beta_{x,y}/\beta_{x,y,0} >$ along the ring. Figure 7 shows the correlation between $< \Delta\beta_x/\beta_{x,0} >$ and $< \Delta\beta_y/\beta_{y,0} >$ in this simulation studies for the above three lattices. In most cases, the horizontal and vertical on-momentum β-beats scale with each other. Therefore, in the following discussion, we will only use the averaged transverse on-momentum β-beat $< \Delta\beta/\beta_0 >$ which is given by $(< \Delta\beta_x/\beta_{x,0} > + < \Delta\beta_y/\beta_{y,0} >)/2$. The changes of second and third order chromaticities are defined by $\Delta\xi_{x,y}^{(2)}/\xi_{x,y,0}^{(2)}$ and $\Delta\xi_{x,y}^{(3)}/\xi_{x,y,0}^{(3)}$.

Table 5: Section contributions to chromatities with 2009 250GeV p-p run Blue ring lattice ($\xi^{(1)}$ corr.)

	$\xi_x^{(1)}$	$\xi_y^{(1)}$	$\xi_x^{(2)}$	$\xi_y^{(2)}$	$\xi_x^{(3)}$	$\xi_y^{(3)}$
IR6	-24.82	-23.33	790.67	1572.9	140726	-8334.45
ARC0608	12.03	9.93	-9.35	160.93	13412	86025
IR8	-24.85	-22.14	1021.77	1415.15	95018.4	8184.07
ARC0810	11.55	10.99	-66.93	-26.64	100199	43998.4
IR10	-4.95	-4.74	-295.57	207.47	-26936.5	-23463.2
ARC1012	12.01	9.9	-56.43	88.28	102326	57822.7
IR12	-4.85	-3.55	-14.57	197.61	-32186.4	-44556.3
ARC1202	11.48	11.01	46.46	-53.54	119750	66446.7
IR2	-4.92	-4.74	-59.7	289.56	-24350.8	-55498.3
ARC0204	12.01	9.89	-60.63	92.89	92814.3	51817.8
IR4	-4.79	-3.56	-254.31	86.03	-27911.5	-7192.21
ARC0406	11.39	11.03	145.99	-35.36	74747.5	41176.6
SUM	1.3	0.69	1187.37	3995.3	627608	216427

Table 6: Section contributions to chromatities with 2011 250GeV p-p run Blue ring lattice ($\xi^{(1)}$ corr.)

	$\xi_x^{(1)}$	$\xi_y^{(1)}$	$\xi_x^{(2)}$	$\xi_y^{(2)}$	$\xi_x^{(3)}$	$\xi_y^{(3)}$
IR6	-27.58	-27.03	966.53	1855.99	170350	-139503
ARC0608	12.97	10.91	39.33	228.84	43877.8	167318
IR8	-28	-25.43	1800.88	1429.85	67221	-127367
ARC0810	12.47	12.22	-138.97	-4.28	130719	16042.4
IR10	-4.17	-4.05	-220.79	93.81	-19229.4	-12078.8
ARC1012	13.02	10.99	-130.38	51.16	152815	30051
IR12	-4.11	-2.76	-106.38	63.88	-29534.9	-27641.9
ARC1202	12.4	12.26	38.07	-66.57	151949	40105.5
IR2	-6.94	-6.86	36.38	413.39	-38680.9	-91579.8
ARC0204	13	10.94	-99.54	62.35	91985.8	34165.9
IR4	-4.02	-2.73	-141.79	-27.22	-12391.4	8677.21
ARC0406	12.25	12.24	159.72	-22.74	47338.6	24241
SUM	1.3	0.7	2203.04	4078.49	756419	-77569.9

Table 7: Section contributions to chromatities with 2010 100GeV Au-Au run Yellow ring lattice ($\xi^{(1)}$ corr.)

	$\xi_x^{(1)}$	$\xi_y^{(1)}$	$\xi_x^{(2)}$	$\xi_y^{(2)}$	$\xi_x^{(3)}$	$\xi_y^{(3)}$
IR6	-22.87	-25.61	765.5	1178.84	118473	80424.3
ARC0604	12.62	11.21	176.28	21.82	171297	131472
IR4	-6.44	-4.76	485.45	-332.93	-117126	-61989.3
ARC0402	12.13	12.36	-13.76	-59.42	157219	99023.1
IR2	-6.34	-6.19	678.84	117.07	-96350.8	-51033.3
ARC0212	12.58	11.23	156.7	-74.35	191960	37037.7
IR12	-6.23	-4.88	596.75	108.87	-91019	-25615.7
ARC1210	11.96	12.38	-60.92	-114.7	152104	86007.5
IR10	-6.46	-6.08	601.32	-305.42	-124078	-52198.7
ARC1008	12.64	11.22	195.08	14.11	184819	126492
IR8	-22.64	-24.28	546.69	985.79	113400	58546.9
ARC0806	11.97	12.43	37.1	16.36	10786.8	14036.1
SUM	2.91	-0.96	4165.07	1556.04	671485	442203

3.2 Results

Figure 8 plots the changes in the second order chromaticities due to the on-momentum β-beat for the above three lattices. In Figures 8, "H" represents the horizontal plane and "V" represents the vertical plane. For

most seeds, when $< \Delta\beta/\beta_0 >$ is below 10%, the second order chromaticity changes are less than 30%. When $< \Delta\beta/\beta_0 >$ is below 20%, the second order chromaticity changes are less then 50%. For the above three lattices, the second order chromaticities without quadrupole errors are all below 4000. Therefore, 10% on-momentum β-beat will introduce maximum of 1200 unit changes to the second order chromaticities. However, for 20% on-momentum β-beat, the second order chromaticities may change the second order chromaticities by 2000 units.

Figures 9 plots the changes in the third order chromaticities due to the on-momentum β-beat for the above three lattices. Although for the most seeds, when the averaged on-momentum β-beat is below 20%, the third order chromaticity changes are less than 50%. However, for some cases with the 2009 and 2011 p-p run Blue lattices, even if the on-momentum β-beat is about 15%, the vertical third order chromaticities are already more than doubled.

3.3 Summary

In summary, for the above three lattices, 10% on-momentum β-beat may introduce 30% changes in second order chromaticities which is about 1200 units. According to the RHIC online second order chromaticity correction experience, to correct 1000-2000 units of second order chromaticity shoul not be very difficult. However, to correct total second order chromaticiies above 4000 units will not be straight-forward if we want to keep more or less balanced strengths among sextupole families and do not want to change the sextupole polarities. With large on-momentum β-beat, the relative phase advances between sextupoles in sextupole families will change too, which in return increases the difficulty in the online correction.

4 Nonlinear chromaticity's dependence on β^*

In this section we investigate the nonlinear chromaticity's dependence on β^* at IP6 and IP8. In this study, the 2009 100 GeV p-p run Blue ring lattices and the 2010 100 GeV Au-Au run Yellow ring lattices are used. The first order chromaticities are corrected to (1,1). In the process of generating these low β^* lattices, we may exceed some power supplies' maximum current limits.

Figures 10 and 11 show the second and third order chromaticities as functions of β^* for the 2009 250 GeV p-p run Blue ring lattices and the 2010 100 GeV Au-Au run Yellow ring lattices. From Figures 10 and 11, the absolute values of second and third order chromaticities increase when the β^*s are decreased. And in most cases, the increase in nonlinear chromaticities with β^* are faster than linear growth. For the 2009 100 GeV p-p run Blue ring lattices, when the β^* is 0.5 m, the vertical second order chromaticity reaches 6000 and the horizontal third order chromaticity reaches 2.5×10^6 . For the 2010 100 GeV Au-Au run Yellow ring lattices, when β^* is 0.65 m, the horizontal second order chromaticity reaches 5500 and the horizontal third order chromaticity reaches 1.0×10^6.

Figure 12 shows the second and third order chromaticities versus β^* for the 2009 250 GeV p-p run Blue ring lattices with second order chromaticity correction. The second order chromaticities are corrected with the 4-knob method [4]. After second order chromaticity correction, the second order chromaticities are significantly reduced. However, the third order chromaticities have small changes.

Figure 13 and 14 shows the percentage contributions from IR6 and IR8 to the first, second, and third chromaticities during β^* squeezing for the 2009 100 GeV p-p run Blue ring lattices and the 2010 100 GeV Au-Au run Yellow ring lattices. With smaller β^*, IR6 and IR8 contribute more percentages to the first order chromaticities. However, their contribution percentages to nonlinear chromaticities do not change significantly.

5 Acknowledgments

We thank J. Bengtsson and C. Gardner for the stimulating discussions during this study.

References

[1] H. Wiedemann, Particle Accelerator Physics, Springer-Verlag, 1995.

[2] J. Bengtsson, *The sextupole scheme for the Swiss Light Source(SLS): an analytical approach*, SLS Note 9/97, March 7, 1997.

[3] S. Tepikian, private communications.

[4] Y. Luo, et al., BNL C-AD AP Note 348, Jan., 2009.

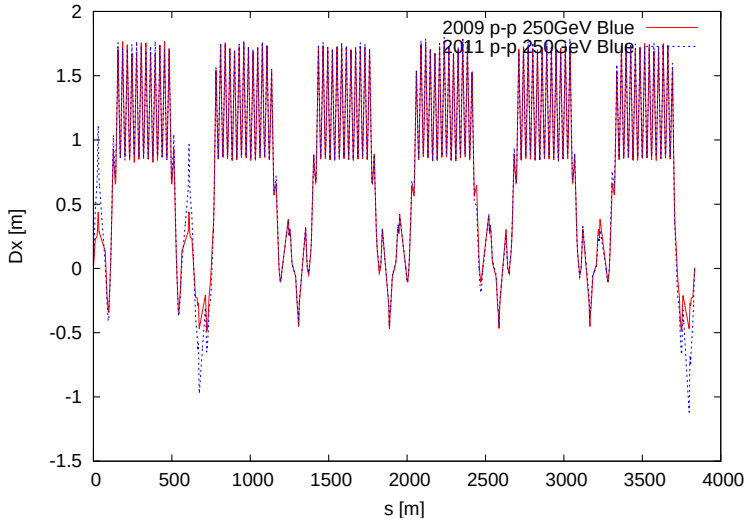

Figure 1: Dispersion along the ring for 2009 and 2011 250GeV p-p run Blue ring lattices.

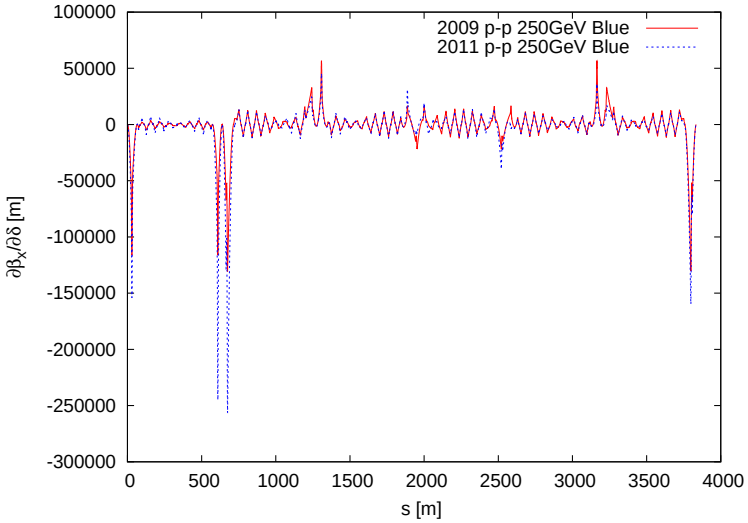

Figure 2: $\frac{\partial \beta_x}{\partial \delta}$ for 2009 and 2011 250 GeV p-p run Blue ring lattices.

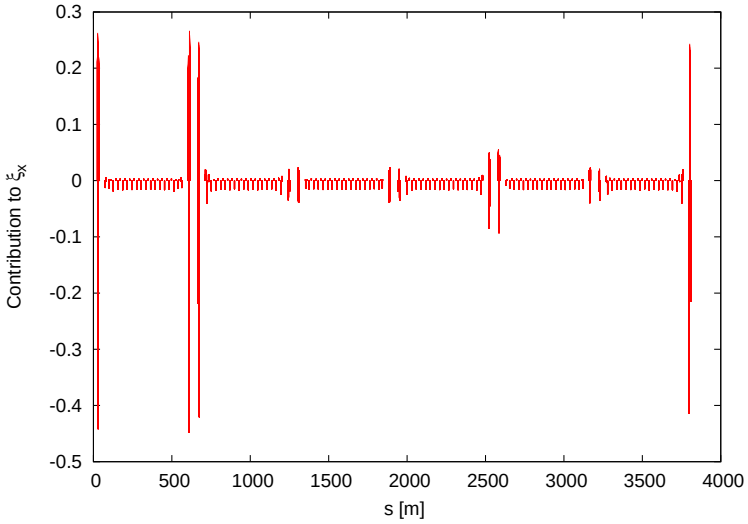

Figure 3: Each element's contribution to $\xi_x^{(1)}$ along the ring for 2011 250 GeV p-p run Blue ring lattice.

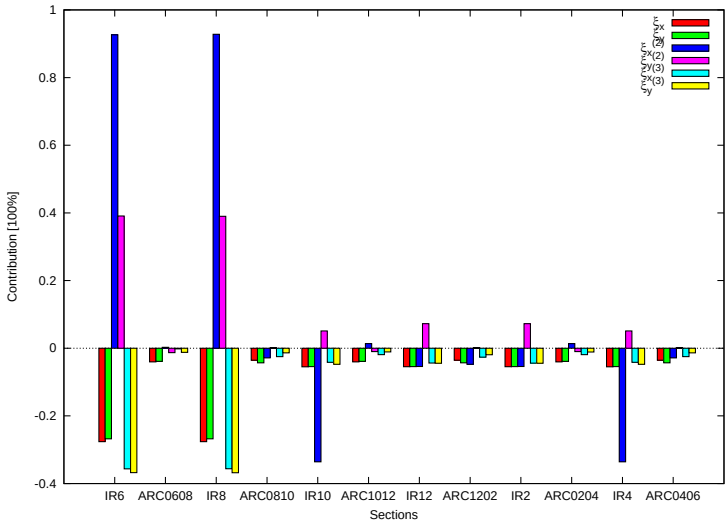

Figure 4: Section contributions to chromatities with 2009 250GeV p-p run Blue ring lattice ($\xi^{(1)}$ uncorr.)

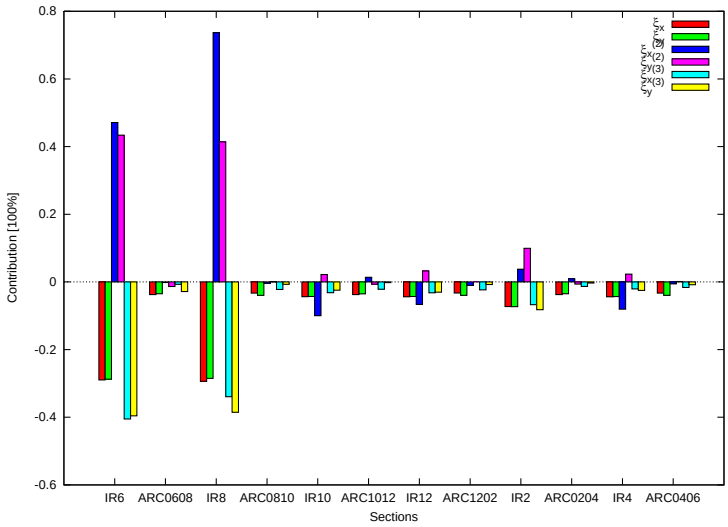

Figure 5: Section contributions to chromatities with 2011 250GeV p-p run Blue ring lattice ($\xi^{(1)}$ uncorr.)

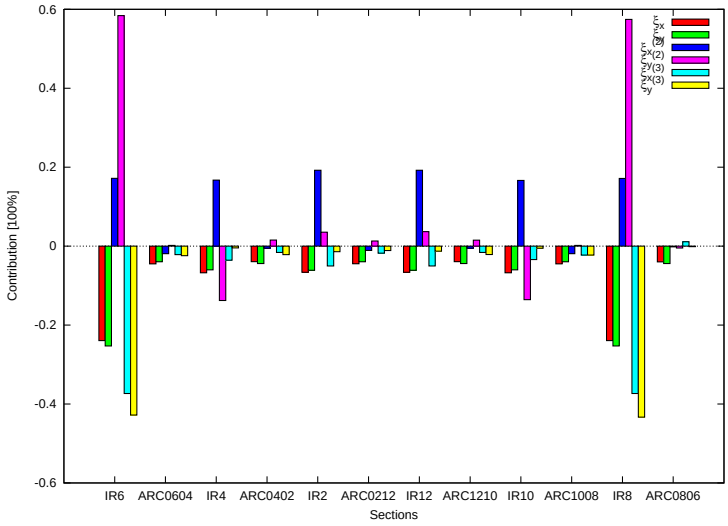

Figure 6: Section contributions to chromatities for 2010 100GeV Au-Au run Yellow ring lattice ($\xi^{(1)}$ uncorr.)

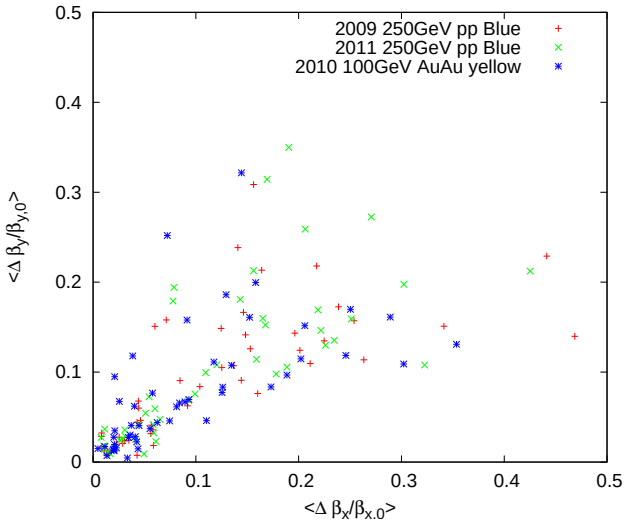

Figure 7: Correlation between $< \Delta\beta_x/\beta_{x,0} >$ and $< \Delta\beta_y/\beta_{y,0} >$ in this simulation studies

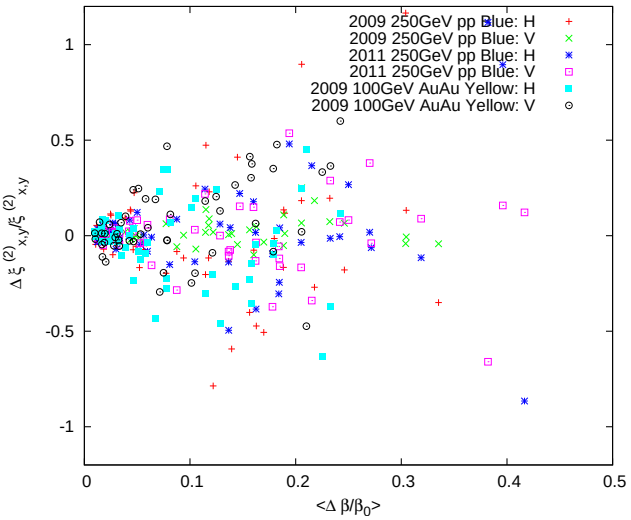

Figure 8: Second order chromaticity changes versus on-momentum β-beat

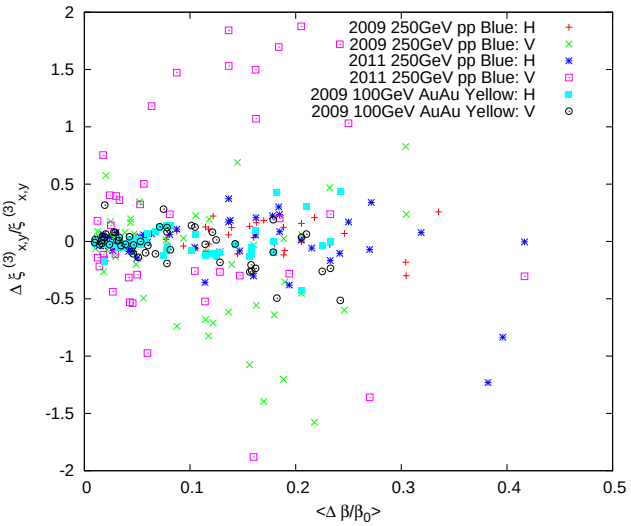

Figure 9: Third order chromaticity changes versus on-momentum β-beat

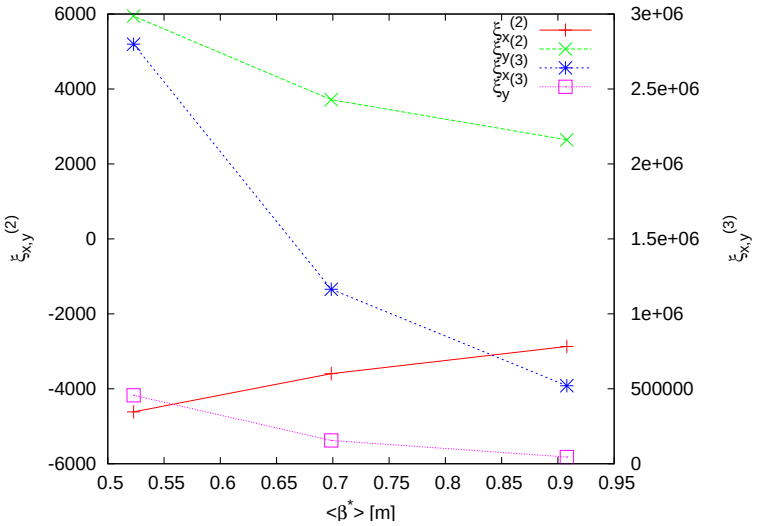

Figure 10: Chromaticities versus β^* for 2009 100 GeV p-p run Blue ring lattices

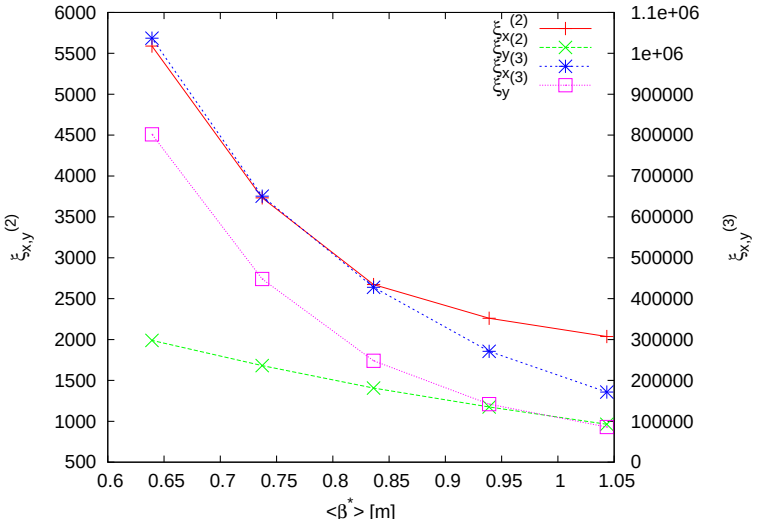

Figure 11: Chromaticities versus β^* for 2010 100 GeV Au-Au run Yellow ring lattices

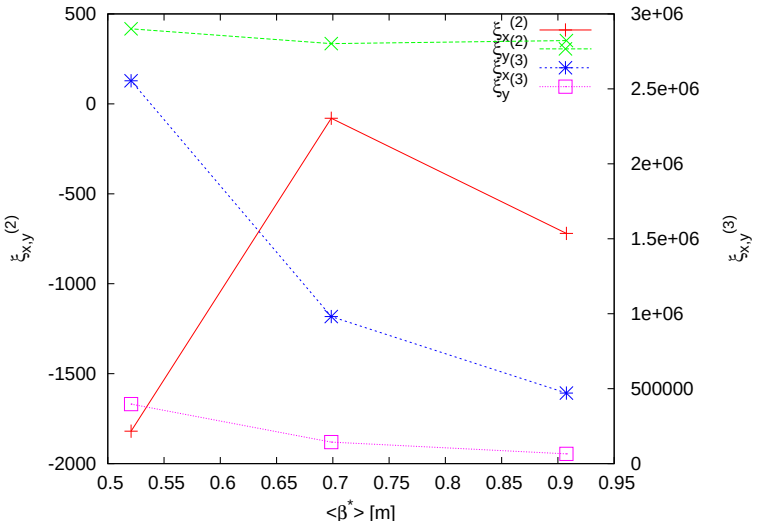

Figure 12: Chromaticities versus β^* for 2009 100 GeV p-p run Blue ring lattices with $\xi^{(2)}$ corrected

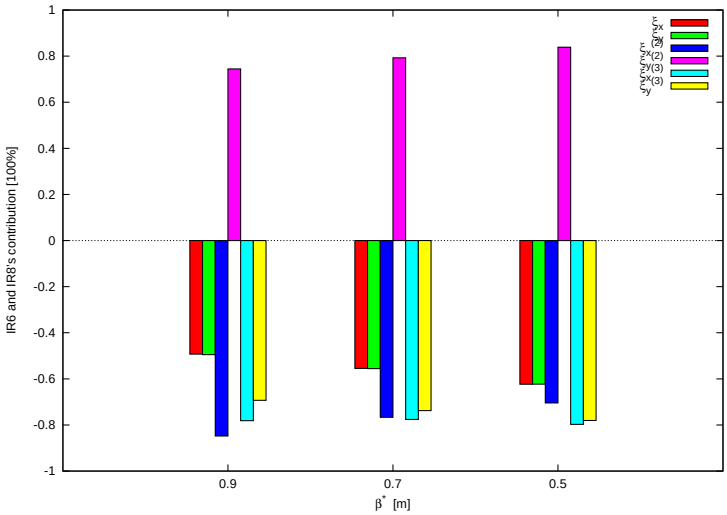

Figure 13: IR6 and IR8's contributions to chromaticities versus β^* at IP6 and IP8 for the 2009 100 GeV p-p run Blue ring lattices

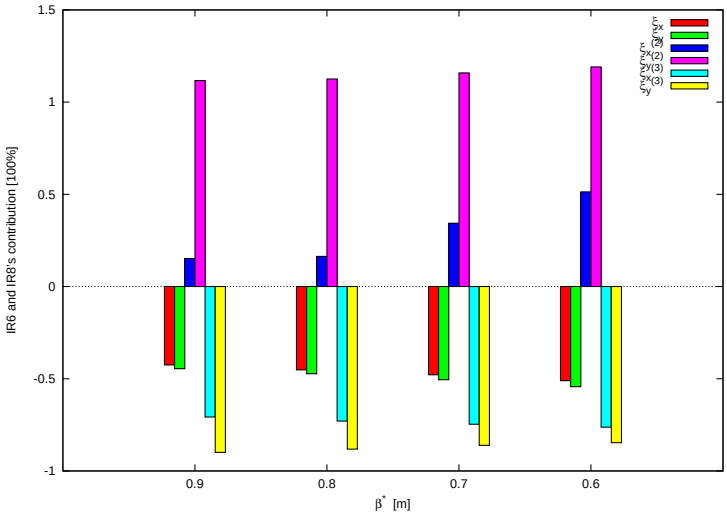

Figure 14: IR6 and IR8's contributions to linear and nonlinear chromaticities versus β^* at IP6 and IP8 for the 2010 100 GeV Au-Au run Yellow ring lattices